

# Rectangular Planar vs Concentric Circular Array for 5G Beamforming

Md Imrul Hasan, *Student Member, IEEE*, and Mohammad Saquib, *Senior Member, IEEE*

**Abstract**—The transmitter signals in the fifth generation (5G) wireless networks suffer from significant path loss due to the use of higher frequencies in Sub-6 GHz and millimeter-wave (mmWave) bands. Therefore, beamforming is an essential and powerful tool in 5G to enhance signal for the desired direction and suppress interferences from other directions. For a given number of antenna elements, the geometry of the array dictates its beam pattern. Most of the works in the existing literature address the use of rectangular planar antenna (RPA) arrays for 5G beamforming. In this work, we demonstrate that a concentric circular antenna (CCA) array is capable of generating a significantly narrower beam than an RPA array while operating with a notably lesser number of antenna elements on a considerably smaller area. This capability of the CCA array can be exploited and utilized in enhancing the performance of a 5G network in both the link and the system levels.

**Index Terms**—5G beamforming, rectangular planar array, concentric circular array, beam packing gain, spatial multiplexing gain, spectral efficiency.

## I. INTRODUCTION

In recent years, with the advent of the internet of things (IoT), and the increasing data rate of media-rich applications, the demand for wireless bandwidth has been expanding very rapidly. The fifth-generation (5G) network employs a large number of antennas, known as massive multiple-input multiple-output (mMIMO) technology, to support the high demand for spectrum [?]. This network uses higher frequencies in Sub-6 GHz (S-band, C-Band, etc.) and millimeter-wave (mmWave) bands, both of which are prone to high path loss. The beamforming technique is an efficient way to handle this issue and thus, incorporated in 5G [1]. The use of mMIMO at mmWave offers narrow beams with high gain and interference suppression capability. These narrow beams also allow spatial multiplexing while increasing the number of user equipments (UEs) for the same time/frequency resources. The narrower the beam, the higher is the antenna-user ratio. Thus, from the system capacity point of view, it is always desirable to maximize that ratio for the same or less number of receiver hardware. On the other hand, for a given number of UEs, having the ability to create more beams enhances the user separation capability which results in a higher signal-to-interference-plus-noise ratio (SINR). Overall, an antenna array capable of offering narrower beams is always desirable.

There exist many types of geometries for 2D antenna arrays. Among those, the rectangular planar antenna (RPA) and the concentric circular antenna (CCA) arrays are the popular ones [2]–[6]. Most of the works in 5G beamforming focus on the use of RPA arrays [2]–[4]. However, CCA arrays also have multiple advantages; the flexibility in array pattern synthesis

and design [6]. In this correspondence item, a framework is developed to identify the best geometry between the RPA and the CCA arrays in the context of 5G beamforming and quantify its performance gain over its counterpart. To the best of our knowledge, no work in the literature has yet performed the above line of inquiry.

There are three methods of implementing antenna beamforming in 5G. Among these, analog beamforming is the simplest and the most cost-effective as it uses minimal amount of software and hardware resources. Here, the output from a single radio frequency (RF) transceiver is passed through the antennas after its phase being adjusted using a phase shifter. Since this system can generate only one signal beam at a time, its effectiveness in 5G is limited. The second type is digital beamforming, where each antenna element is supplied by its own RF transceiver, and each signal is offered phase modifications in baseband processing before the transmission. Hence, this beamforming allows several sets of beams to be generated which is ideal for 5G networks. However, since several hundred of antenna elements are possible in these networks, signal processing/hardware complexities, and high power/area requirements make digital beamforming prohibitively expensive. The last one is hybrid beamforming, which is introduced in 5G as a possible solution to the above limitations. In hybrid beamforming, analog beamforming is carried out in the RF stage combining with digital precoding which integrates the flexibility of the digital beamforming with the simplicity of the analog beamforming. Hence, in this work, we concentrate on the hybrid beamforming method while comparing the performance between the RPA and the CCA arrays.

The rest of the correspondence item is organized as follows: Section II provides the antenna array models. In Section III, different beamforming performance criteria are illustrated. Section IV contains the numerical study, and finally, the concluding remarks are presented in Section V.

## II. ANTENNA ARRAY MODEL

In 5G networks, the use of mmWave allows a large number of antenna elements within a small area of an array. Let's provide the mathematical model of a 2D RPA array first assuming the desired signal of wavelength  $\lambda$  impinges upon the array from the elevation angle  $\theta_0$  and the azimuthal angle  $\phi_0$ .

### A. RPA Array

A dedicated 2D RPA array for the desired UE consists of  $N_x \times N_y$  omni-directional elements placed along a rectangular

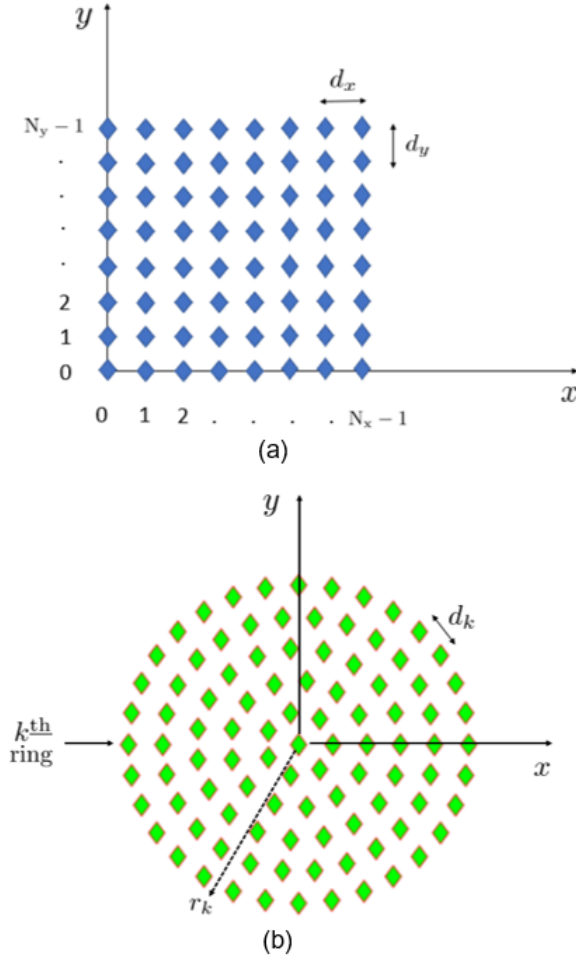


Fig. 1. a) RPA array geometry, b) CCA array geometry.

grid in such a way that every row and column parallel to the  $x$ , and  $y$  axis has  $N_x$ , and  $N_y$  elements, respectively. This array structure is shown in Fig. 1 (a), where the element spacing corresponding to every row and column is denoted by  $d_x$ , and  $d_y$ . The overall beam pattern of the RPA array towards the desired user is obtained by [7]

$$F_{\text{RPA}}(\theta, \phi) = \sum_{m=0}^{N_x-1} \sum_{n=0}^{N_y-1} A_{mn} e^{i(2\pi/\lambda)\{m \times h(\theta, \phi) + n \times g(\theta, \phi)\}}, \quad (1)$$

where  $A_{mn}$  denotes the beamformer weight along the  $m^{\text{th}}$  row and  $n^{\text{th}}$  column,

$$h(\theta, \phi) = d_x (\sin \theta \cos \phi - \sin \theta_0 \cos \phi_0),$$

and

$$g(\theta, \phi) = d_y (\sin \theta \sin \phi - \sin \theta_0 \sin \phi_0).$$

Next, we describe the beam pattern of the CCA array.

### B. CCA Array

The geometry of a CCA array is depicted in Fig. 1 (b), where the  $i^{\text{th}}$  ring in the array with a radius  $r_i$ , contains  $N_i$  omni-directional elements, where  $i = 1, 2, \dots, k$ . If  $d_i$

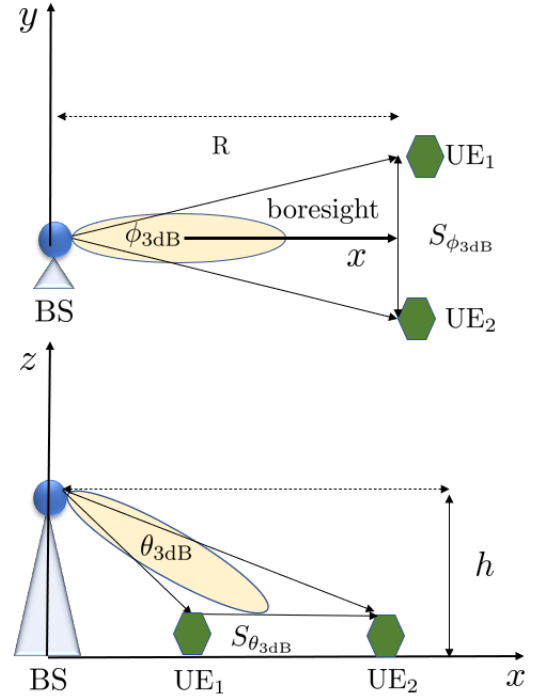


Fig. 2. Inter-UE spatial separation in 2D.

denotes the inter-element distance in the  $i^{\text{th}}$  ring, then  $d_i = 2r_i \sin(\pi/N_i)$ . The array factor of the CCA directed towards  $(\theta_0, \phi_0)$  is given by [8]

$$F_{\text{CCA}}(\theta, \phi) = 1 + \sum_{i=1}^k \sum_{j=1}^{N_i} B_{ij} e^{i(2\pi r_i/\lambda) f_{ij}(\theta, \phi)}, \quad (2)$$

where  $B_{ij}$  the beamformer weight for the  $j^{\text{th}}$  element in the  $i^{\text{th}}$  ring,

$$f_{ij}(\theta, \phi) = \sin \theta \cos(\phi - \phi_{ij}) - \sin \theta_0 \cos(\phi_0 - \phi_{ij}),$$

and  $\phi_{ij} = 2\pi(j-1)/N_i$ .

Recall that, our objective is to compare the performance between the RPA and the CCA arrays using the hybrid beamforming technique. Let's assume, the two array configurations shown in Fig. 1 (a)-(b) are obtained for the desired UE by incorporating a digital precoding. The purpose of this precoding is to distribute the total number of hardware resources evenly among all the UEs. The analog part of the hybrid beamforming is then modeled by assuming uniform illumination for both the arrays and letting all the element weights  $A_{mn}$  in (1) and  $B_{ij}$  in (2) to be equal to 1 as in [7].

### III. BEAMFORMING PERFORMANCE CRITERIA

In 5G networks, the beam formed by a base station (BS) using a large-scale antenna array becomes very narrow to provide extremely high directional selectivity and array gain [9]. This narrow beam facilitates more user UEs within the same spatial dimension in a wireless ultra-dense network. To evaluate how densely we can allow beams to support neighboring UEs, the idea of beam packing is explored considering

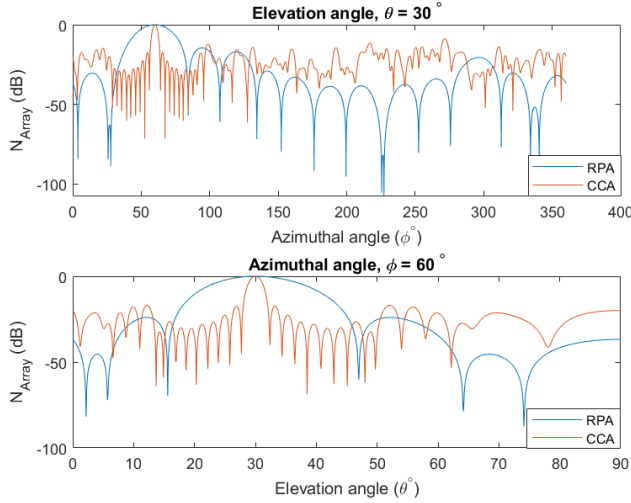


Fig. 3. Beam patterns for the RPA and the CCA arrays.

an arbitrary sphere around the BS. This number is calculated by the maximum number of supported half-power beamwidths (HPBW) in the elevation ( $\theta_{3dB}$ ), and the azimuthal ( $\phi_{3dB}$ ) direction. The overall beam packing gain of the CCA array over the RPA array can be defined as

$$G_{BP} = \frac{\theta_{3dB\ RPA} \phi_{3dB\ RPA}}{\theta_{3dB\ CCA} \phi_{3dB\ CCA}}. \quad (3)$$

The above gain measures the user ratio served by the CCA array to the RPA array in 3D for given system resources. This gain is useful while comparing two systems in terms of the maximum number of supportable UEs. As the HPBW depends on the number of elements and their placement in the array, this gain varies for different array configurations.

Next, we relate the above angular HPBW separation into UE separation distances on both the vertical and the horizontal planes. As shown in Fig. 2, these distances can be approximated as [10]

$$S_{\theta_{3dB}} = R - h \tan\{\arctan(R/h) - \theta_{3dB}\}, \quad (4)$$

and

$$S_{\phi_{3dB}} = 2R \tan\{\phi_{3dB}/2\}, \quad (5)$$

where  $R$  is the BS range and  $h$  is the BS height. Based on these distances, another spatial multiplexing gain that a CCA array has over an RPA array can be calculated using

$$G_{SM} = \frac{S_{\theta_{3dB\ RPA}} S_{\phi_{3dB\ RPA}}}{S_{\theta_{3dB\ CCA}} S_{\phi_{3dB\ CCA}}}. \quad (6)$$

The above gain in (6) states how many times more number of UEs can be supported on a plane at distance  $R$  away from the BS using a CCA array instead of an RPA array. Note that all these separation schemes prohibit the beam from overlapping while suppressing the interference from any undesired direction.

Now, in order to analyze the quality of signals in 5G networks, we evaluate the SINR which is given by [11]

$$\text{SINR} = \frac{P}{I + N}, \quad (7)$$

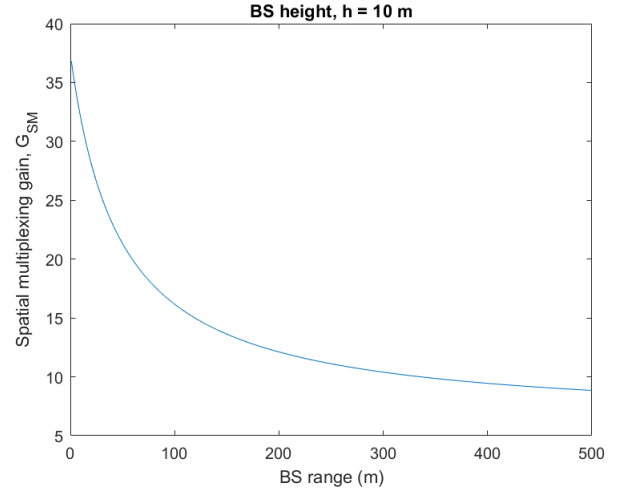


Fig. 4. Spatial multiplexing gain of the CCA array over the RPA array.

where  $P$  is the received power of the signal of interest,  $I$  is the interference power of the other (interfering) signals in the network, and  $N$  is the average power of the background noise. In general, the desired signal, interference, and noise signals are mutually statistically independent. This SINR is directly related to the information data rate transmitted over a given bandwidth ( $W$  Hertz (Hz)). The maximum achievable user data rate can be obtained from Shannon's capacity formula [12] as

$$C = W \log_2 \left( 1 + 10^{0.1(\text{SINR} - \gamma)} \right) \text{ bits/second (bps)}, \quad (8)$$

and the corresponding spectral efficiency is

$$\rho = \log_2 \left( 1 + 10^{0.1(\text{SINR} - \gamma)} \right) \text{ bps/Hz}, \quad (9)$$

where the SINR is in dB and  $\gamma$  denotes the loss factor.

#### IV. NUMERICAL STUDY

In order to have a fair comparison, the area size and the number of elements should be the same for both the RPA and the CCA arrays. However, the difference in the shape of the geometries and the inter-element spacing requirement do not allow meeting both the criteria simultaneously. To emphasize the performance of the CCA array, we force its area size to be less than that of the RPA array and write from Section II,

$$\pi r_k^2 < (N_x - 1)(N_y - 1)d_x d_y. \quad (10)$$

Considering the equal inter-ring distance (i.e.  $r_i = ir_1$ ), we find the number of rings in a CCA array,

$$k < \sqrt{\frac{(N_x - 1)(N_y - 1)d_x d_y}{\pi r_1^2}} = \sqrt{\frac{(N_x - 1)(N_y - 1)}{\pi}}, \quad (11)$$

where the rightmost equality is obtained using  $d_x = d_y = r_1 = \lambda/2$ . Since  $k$  must be an integer, we choose the largest integer value of  $k$  that satisfies inequality (11). The number of elements on the  $i^{\text{th}}$  ring of the CCA array is  $N_i = \lceil \pi / \arcsin\left(\frac{d_i}{2r_i}\right) \rceil$ , where  $i = 1, 2, \dots, k$ ,  $d_i = \lambda/2$  and

$\lceil \cdot \rceil$  denotes the ceiling function. Hence, the total number of antenna elements in the CCA array is  $N_{CCA} = \sum_{i=1}^k N_i$ . We will shortly see that guaranteeing inequality (10) (i.e. the area size of the CCA array is less than that of the RPA array in a 5G network) warrants  $N_{CCA} < N_{RPA}$ , where  $N_{RPA} = N_x N_y$  denotes the total number elements in the RPA array.

The remaining part of this section contains the numerical examples demonstrating the beamforming performance comparison between the two arrays of interest for a 5G network.

### A. Numerical Results

Here, our objectives are 1) to perform a comparative study between the RPA, and the CCA arrays on the system level using (3) and (6), and 2) to provide insights into the link level performance of the arrays using (7), and (9). Assume, the frequency of interest is 28 GHz band. For the RPA beamforming, we consider  $N_x = N_y = 10$  (i.e.  $N_{RPA} = 100$ ). As for the CCA, we use  $k = 5$ , and  $N_{CCA} = 97$ . These are our network parameters of interest unless otherwise specified.

Consider the signal of interest is at  $(\theta_0, \phi_0) = (30^\circ, 60^\circ)$ . Now, we evaluate the normalized beam pattern of the arrays defined by [12]

$$N_{array}(\theta, \phi) = 20 \log_{10} (|F_{array}(\theta, \phi)| / |F_{array}(\theta_0, \phi_0)|), \quad (12)$$

which are presented in Fig.3 for variable azimuthal, and elevation angles. Here, it can be noticed that the CCA array produces significantly narrower beams with relatively higher side lobes at distant angles. Using these figures, we also calculate the HPBW for the RPA  $(\theta_{3dB}, \phi_{3dB}) = (12^\circ, 20.7^\circ)$ , and for the CCA,  $(\theta_{3dB}, \phi_{3dB}) = (2^\circ, 3.4^\circ)$ . Using (3), we obtain the beam packing gain of the CCA over the RPA array as  $G_{BP} \approx 36$ . This result suggests that in a 3D space, a 5G network equipped with this CCA array is expected to serve 36 times more UEs than the above RPA array while operating with 3% less number of antenna elements. Considering a square RPA array and varying  $N_{RPA}$  from 9 to 256, this beam packing gain is listed in Table I. Notice that the beam packing gain,  $G_{BP}$  offered by the CCA array is always significant while operating with a considerably lesser number of antenna elements on substantially smaller area size. Trade-offs among the beam packing, element and area gains are also observed in Table I; see  $G_{BP} = 30.34$  when element gain = 19.75%, area gain = 37.94% and  $G_{BP} = 36.53$  when element gain = 3%, area gain = 21.46%.

In the next numerical example, our goal is to observe the spatial multiplexing gain on a plane as a function of the BS range using (6); see Fig. 4, where we use the practical BS ranges suggested for 5G systems [13]. Here, it can be noticed that the multiplexing gain of the CCA array is always significant; it varies from 36 to 8. As expected, in the vicinity of the BS, the multiplexing gain is close to the beam packing gain and diminishes with the increase of the BS range.

Finally, we want to compare the maximum spectral efficiency offered by the two arrays of interest. We assume all the UEs are distributed within  $0^\circ$  to  $90^\circ$  in both the planes (azimuthal and elevation). We find that a fully-loaded network with a CCA array (namely Network 1) can accommodate

TABLE I  
TRADE-OFFS AMONG THE BEAM PACKING, ELEMENT, AND AREA GAINS

$k$	No. of elements		Element Gain (%)	Area Gain (%)	$G_{BP}$
	CCA	RPA			
1	7	9	22.22	65.09	27.76
2	20	25	20.00	49.73	29.51
3	39	49	20.40	42.30	29.73
4	65	81	19.75	37.94	30.34
5	97	100	3.00	21.46	36.53
6	135	144	6.25	21.46	35.83
7	179	196	8.67	21.46	34.97
8	230	256	10.16	21.46	36.65

t

TABLE II  
PERFORMANCE ON THE AZIMUTHAL PLANE

Network Type	Array	SINR (dB)	$\rho = C/W$ (bps/Hz)
Network 1	CCA	8.01	2.43
	RPA	-7.26	0.18
Network 2	CCA	16.12	4.87
	RPA	11.12	3.31

TABLE III  
PERFORMANCE ON THE ELEVATION PLANE

Network Type	Array	SINR (dB)	$\rho = C/W$ (bps/Hz)
Network 1	CCA	6.44	2.02
	RPA	-7.20	0.18
Network 2	CCA	18.4	5.61
	RPA	10.51	3.13

approximately 26 UEs on the azimuthal and 45 UEs on the elevation plane based on the number of non overlapping beams. Whereas, in a fully loaded network with an RPA array (namely Network 2), those numbers are 4 and 7, respectively. For those 4 network scenarios, SINR, and the user spectral efficiency ( $\rho$ ) are listed in Table II, and III for performance comparison. Here, we have considered SNR = 20 dB, and loss factor  $\gamma = 1.6$  dB [12]. Notice that in Network 2, where the use of the RPA array is feasible, the CCA array is capable of providing 1.47 times and 1.79 times spectral efficiency gain over the RPA array on the elevation and azimuthal planes, respectively. As expected, these gains are significantly more in Network 1 (13.5 and 11.22 times, respectively), where the RPA array is forced to operate at a very poor SINR owing to allowing a significant amount of interferences inside the desired beam.

### V. CONCLUSIONS

In this correspondence item, we presented a comprehensive analytical framework to compare the beamforming performance between the RPA and the CCA arrays for 5G and beyond wireless networks. Our numerical study demonstrated that in a 5G network, the CCA array significantly outperforms the RPA array operating with a lesser number of antenna elements on a smaller area size. For instance, a CCA array with 97 antenna elements offered approximately 36 times beam packing gain, 21 times spatial multiplexing gain at  $R = 50$  m, and depending on the number of UEs, user spectral efficiency gain can be up to 13.5 times on the azimuthal plane over a  $10 \times 10$  RPA array.

## REFERENCES

- [1] A. Simonsson, M. Thurfjell, B. Halvarsson, J. Furuskog, S. Wallin, S. Itoh, H. Murai, D. Kurita, K. Tateishi, A. Harada *et al.*, "Beamforming gain measured on a 5g test-bed," in *2017 IEEE 85th Vehicular Technology Conference (VTC Spring)*. IEEE, 2017, pp. 1–5.
- [2] T. Varum, A. Ramos, and J. N. Matos, "Planar microstrip series-fed array for 5g applications with beamforming capabilities," in *2018 IEEE MTT-S International Microwave Workshop Series on 5G Hardware and System Technologies (IMWS-5G)*. IEEE, 2018, pp. 1–3.
- [3] U. Rafique and H. Khalil, "Modified planar rectangular antenna array for wideband 5g mimo applications," in *2019 International Conference on Advances in the Emerging Computing Technologies (AECT)*. IEEE, 2020, pp. 1–5.
- [4] S. Krishna, G. Mishra, and S. K. Sharma, "A series fed planar microstrip patch array antenna with 1d beam steering for 5g spectrum massive mimo applications," in *2018 IEEE Radio and Wireless Symposium (RWS)*. IEEE, 2018, pp. 209–212.
- [5] M. Reza, M. Hossain, and M. Rashid, "Robust centered element concentric circular antenna array with low side lobe using variable loading and tapering windows in the presence of array imperfections," *International Journal of Antennas and Propagation*, vol. 2017, 2017.
- [6] M. I. Dessouky, H. Sharshar, and Y. Albagory, "Efficient sidelobe reduction technique for small-sized concentric circular arrays," *Progress In Electromagnetics Research*, vol. 65, pp. 187–200, 2006.
- [7] W. Li, X. Huang, and H. Leung, "Performance evaluation of digital beamforming strategies for satellite communications," *IEEE Transactions on Aerospace and Electronic systems*, vol. 40, no. 1, pp. 12–26, 2004.
- [8] B. Hamdi, S. Limam, and T. Aguil, "Uniform and concentric circular antenna arrays synthesis for smart antenna systems using artificial neural network algorithm," *Progress In Electromagnetics Research B*, vol. 67, pp. 91–105, 2016.
- [9] S. Chen, S. Sun, G. Xu, X. Su, and Y. Cai, "Beam-space multiplexing: Practice, theory, and trends, from 4g td-lte, 5g, to 6g and beyond," *IEEE Wireless Communications*, vol. 27, no. 2, pp. 162–172, 2020.
- [10] G. Fokin, S. Bachevsky, and V. Sevidov, "System level performance evaluation of location aware beamforming in 5g ultra-dense networks," in *2020 IEEE International Conference on Electrical Engineering and Photonics (EExPolytech)*. IEEE, 2020, pp. 94–97.
- [11] J.-J. Park, B.-J. Bae, and T.-G. Chang, "Investigation of the sinr behavior of the beamforming-applied cellular cdma base station receiver," in *WCNC. 1999 IEEE Wireless Communications and Networking Conference (Cat. No. 99TH8466)*, vol. 2. IEEE, 1999, pp. 688–692.
- [12] M. Salah and I. Kostanic, "Performance evaluation of 5g downlink under different beamforming and scheduling methods," in *2019 IEEE 9th Annual Computing and Communication Workshop and Conference (CCWC)*. IEEE, 2019, pp. 0778–0782.
- [13] viavisolutions.com, "What is 5G Technology?" [Online]. Available: <https://www.viavisolutions.com/en-us/5g-technology> [Accessed: 02- August- 2021].